Polymer 51 (2010) 5910–5920

Contents lists available at ScienceDirect

Polymer

journal homepage: www.elsevier.com/locate/polymer

Functional coatings for anti-biofouling applications by surface segregation of block copolymer additives

Eva Berndt [a], Sven Behnke [a], Astrid Dannehl [b], Aleksandra Gajda [a], Jost Wingender [b], Mathias Ulbricht [a,*]

[a] Lehrstuhl für Technische Chemie II, Universität Duisburg-Essen, 45141 Essen, Germany
[b] Biofilm Centre, Lehrstuhl für Aquatische Mikrobiologie, Universität Duisburg-Essen, Geibelstraße 41, 47057 Duisburg, Germany

ARTICLE INFO

Article history:
Received 26 July 2010
Received in revised form
30 September 2010
Accepted 3 October 2010
Available online 12 October 2010

Keywords:
Block copolymers
Surface functionalization
Polymer films and coatings

ABSTRACT

Temperature responsive or bactericidal coatings with poly(*n*-butyl methacrylate) (PBMA) as bulk material and surface segregated poly(*n*-butyl acrylate)-*block*-poly-(*N*-isopropylacrylamide) (PBA-*b*-PNIPAAm) or poly(*n*-butyl acrylate)-*block*-quaternized poly(2-(dimethylamino)ethyl methacrylate) (PBA-*b*-PDMAEMAq) as additive were prepared via sequential solvent evaporation of polymer solutions in a solvent mixture. The degree of enrichment at the air surface of the coating and the functionality were examined for different molecular weight additives with different block ratios obtained via Atom Transfer Radical Polymerization (ATRP). The design of the block copolymers with an anchor block (PBA) which is compatible with the bulk polymer (PBMA) and water-compatible functional blocks (PNIPAAm and PDMAEMAq) along with the selection of suited solvent mixtures based on pre-estimation of the selective solubility and sequential evaporation via the Hansen solubility parameters and vapor pressures, respectively, were found to work very well. A small fraction of water in the solvent mixture had been crucial to obtain surface segregation of the functional block, e.g., a PNIPAAm surface with temperature-switchable wettability. Reversible temperature dependent wettability and long term stability of the functionalization, based on contact angle data, were obtained for an optimized PBA-*b*-PNIPAAm additive. Surface charge density, estimated from dye binding and zeta potential measurements, and killing efficiency against *Staphylococcus aureus* were investigated for PBA-*b*-PDMAEMAq as additive. Both block copolymer additives were found to dominate the surface properties and the functionality of the PBMA coating.

1. Introduction

The performance of many materials in diverse applications does not only depend on their bulk properties but benefits additionally from their surface composition, microstructure and functionality [1]. Examples for technologically important applications that are affected by a coating's surface properties include wetting, adhesion and adsorption tendencies and, consequently, biocompatibility and fouling resistance. A process that is selective with respect to incorporation of a functional additive in the surface region of a coating and at the same time leaves its bulk properties intact is anticipated to improve the performance of many materials.

The surface properties of a polymeric material can be modified by physical (non-covalent) or chemical (covalent) functionalization techniques such as "grafting to" or "grafting from" of layers from another polymer [2]. In contrast to these post-treatment techniques, Bergbreiter et al. introduced a process named entrapment functionalization in which a block cooligomer is blended with a bulk polymer and, due to its surface selectivity, the additive is located at the casted film's air surface after solvent evaporation [3,4]. They claim this strategy to result in a stable functionalization and observed enhanced surface selectivity for low contents of the additive and for higher molecular weight additives. There is still a discussion whether the surface enrichment of the additive is driven by the surface free energy differences between the additive and the bulk material or whether the configurational entropy per segment of polymer chains near rigid surfaces is substantially lower than in bulk polymer systems, a theory in which low molecular weight polymers would be preferentially located at the film's surface [4–7]. Nevertheless, this approach to obtain surface segregated films by adding small amounts of block copolymer architectures has been applied especially for low surface energy polymers (e.g., poly(dimethylsiloxane)) [8–10]. Recently the use of block copolymers containing poly(ethylene oxide) blocks that accumulate at the air interface of the coating was investigated in terms of fouling resistance and blood compatibility [11,12]. Still for most of the blends

* Corresponding author. Tel.: +49 201 183 3151; fax: +49 201 183 3147.
E-mail address: mathias.ulbricht@uni-due.de (M. Ulbricht).

0032-3861/$ – see front matter © 2010 Elsevier Ltd. All rights reserved.
doi:10.1016/j.polymer.2010.10.002

a post-treatment step such as annealing of the films above the glass transition temperature of the bulk polymer is necessary or enhances surface segregation to a certain extent. However, this procedure is not practically applicable in all circumstances. It has been shown that the casting solvent in sample preparation significantly affects the surface segregation already during the preparation process [8,13].

In this paper we present a concept which is based on the selective evaporation of different solvents with different abilities to dissolve the bulk polymer and the functional additive to result in functional coatings with temperature responsive or bactericidal surface properties. As additives two different well defined functional block copolymer architectures were used. To obtain a temperature responsive material poly(*n*-butyl acrylate)-*block*-poly(*N*-isopropylacrylamide) (PBA-*b*-PNIPAAm; cf. Fig. 1a) was added to poly(*n*-butyl methacrylate) (PBMA) as bulk material. The composition of the additive was chosen so that PBA acts as an anchor block which is, due to its chemical similarity to the bulk material, able to firmly entangle in the coating's bulk polymer and result in a stable functionalization (Fig. 1b). The additive was synthesized applying Atom Transfer Radical Polymerization (ATRP) to result in low molecular weight distribution architectures [14]. As ATRP of BA is well known in literature, but PBA has a low glass transition temperature, it was chosen as anchor block. PBMA with its higher glass transition temperature exhibits very good film forming properties and thus was chosen as bulk material.

The polymers were dissolved in a mixture of ethyl acetate (EtOAc), *n*-propanol (*n*-PrOH) and water. These solvents exhibit selective properties for these polymers which were pre-estimated by the values of the Hansen parameters: EtOAc is able to dissolve the bulk polymer and both blocks of the additive, *n*-PrOH and water only exhibit a good solubility for the functional block PNIPAAm (Fig. 2). As EtOAc will evaporate firstly (vapor pressure: 9733 Pa), selective precipitation of the bulk PBMA and the anchor block PBA is anticipated to occur. The residual water (vapor pressure: 3166 Pa) and *n*-PrOH (vapor pressure: 1987 Pa) will be still present at the air

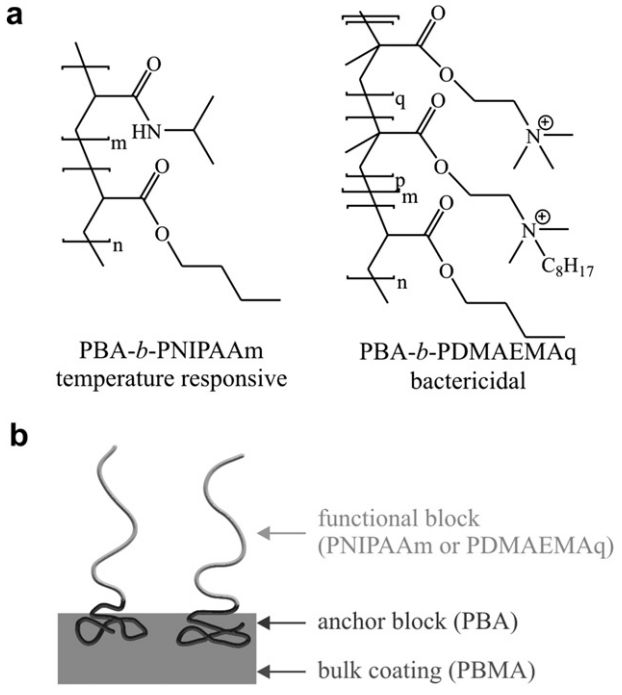

Fig. 1. (a) Block copolymers used as additives in this study with a temperature responsive block PNIPAAm or a bactericidal block PDMAEMAq; (b) schematic description of surface segregation of the functional block copolymers as additives at the air interface of the bulk coating.

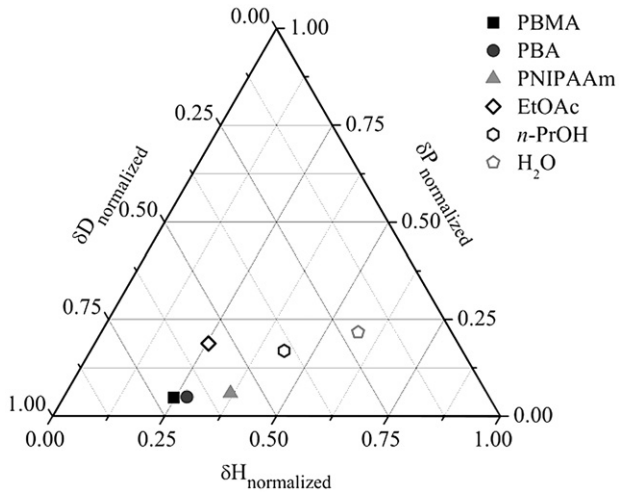

Fig. 2. Hansen solubility parameters used for the pre-estimation of the selective solubility of the polymers [19–21]; values for the energy from hydrogen bonds (δH), from polar bonds (δP) and from dispersion bonds (δD) are normalized.

interface of the slowly forming polymer coating thereby inducing selective migration of the soluble PNIPAAm block to this interface. After solvent evaporation a functionalized surface with temperature responsive properties is obtained (cf. Fig. 1b). Similar PNIPAAm-containing materials have been proposed to exhibit anti-fouling properties due to their reversible transition in wettability and swelling upon changing the temperature around the lower critical solution temperature (LCST) of about 32 °C [15–18]. The influences of molecular weight of the block copolymer and the block ratios on surface segregation were characterized and the long term stability of the coating with the optimal additive was determined.

Additionally, poly(*n*-butyl acrylate)-*block*-quaternized poly(2-(dimethylamino)ethyl methacrylate) (PBA-*b*-PDMAEMAq; cf. Fig. 1a) was synthesized via ATRP and used as additive for coatings applying the approach described above (cf. Fig. 1b). This polymer is anticipated to exhibit bactericidal properties due to the contact active destruction of microbial cell membranes by the hydrophobically quaternized DMAEMA chains [22,23]. The killing efficiency of the resulting functional surfaces against *Staphylococcus aureus* was determined for additives with different molecular weights. Overall, a versatile generic approach for the preparation of functional coatings with long term stability due to the additive's architecture by adding a small amount of a block copolymer to a bulk polymer and sequential evaporating of selective solvents is presented.

2. Experimental section

2.1. Materials

N-Isopropylacrylamide (NIPAAm; Acros Organics, 99%, stabilized) was recrystallized twice from *n*-hexane (Acros, p.a.), dried in vacuum and stored at 4 °C; *n*-Butyl acrylate (BA; Fluka, ≥99%, stabilized), *n*-butyl methacrylate (BMA; Fluka, 99%, stabilized) and 2-(dimethylamino)ethyl methacrylate (DMAEMA; Polyscience) were dried over CaH_2 (Fluka, ≥97%), distilled under reduced pressure and stored under argon at 4 °C; α,α′-Azoisobutyronitrile (AIBN, Fluka, ≥98%) was recrystallized from methanol prior to use. Tris (2-(dimethylamino)ethyl)amine (Me_6TREN) was synthesized according to the literature [24]. 1,1,4,7,10,10-Hexamethyltriethylenetetramine (HMTETA, 97%) and CuBr (99.999%) from Aldrich, CuCl (99.99%), 1-bromooctane (99%), toluene and *n*-propanol (p.a.) from Acros Organics, *N*,*N*-dimethylformamide (DMF) from Normapur

(p.a.), ethyl α-bromoisobutyrate (EBriB, ≥ 97.0%), *N,N,N′,N′,N″*-pentamethyldiethylenetriamine (PMDETA, ≥98%), methanol (p.a.) from Fisher Scientific, iodomethane (≥99%) and ethyl acetate (p.a.) from Fluka, and *n*-heptane (p.a.) from AppliChem were used as received. Argon was used throughout all syntheses which are sensitive to oxygen. Column isolation of copper was performed using activated neutral aluminum oxide from Acros Organics. For the determination of cell membrane integrity of *S. aureus* the LIVE/DEAD *Bac*Light Bacterial Viability Kit L7012 from Invitrogen was used. For production of ultra pure water a Milli-Q system from Millipore was used to result in Milli-Q water with a conductivity of 18 M Ω.

2.2. Synthesis

2.2.1. General procedure for ATRP of the functional additives (PBA-b-PNIPAAm and PBA-b-PDMAEMAq)

The polymerizations of BA and NIPAAm were conducted according to literature [25]. Briefly, for the macroinitiator synthesis BA (c(BA) = 7 mol/L), DMF and PMDETA were introduced to a three neck flask. The solution was degassed for 30 min and CuBr was added. After degassing for another 10 min the polymerization was started by adding the degassed initiator EBriB. Immediately, the flask was immersed in an oil bath preheated at 50 °C. After 45 min (for #4 and #7) or 150 min (for #6) the polymerization was stopped by addition of THF, the catalyst was removed by passing the solution through an aluminum oxide column, the polymer was precipitated in MeOH:H_2O, 1:1, and dried in an oven at 60 °C overnight. PBA macroinitiators for block copolymers #1, #2, #3 and #5 were synthesized using Me_6TREN as ligand and CuCl as catalyst (for exact conditions see Ref. [25]).

For the synthesis of temperature responsive block copolymers (#1–#5; Table 1) a three neck flask was charged with NIPAAm (final concentration: c(NIPAAm) = 3.9 mol/L), Me_6TREN and DMF and degassed with argon for 30 min. At the same time the macroinitiator (PBA, obtained via ATRP as described above) was dissolved in DMF and the solution was degassed for 30 min. CuCl was added to the monomer solution, and the complex was formed for another 10 min. The macroinitiator was added via a syringe, and the flask was placed in an oil bath preheated at 25 °C. After 60 min (for #1), 120 min (for #2 and #3), 300 min (for #4) or 180 min (for #5) the polymerization was stopped by addition of THF and the solution was filtered through an aluminum oxide column. The resulting block copolymer was precipitated in MeOH:H_2O, 1:1, and additionally in heptane. The filtered product was dried in an oven overnight.

For the synthesis of the cationic block copolymers (#6 and #7; Table 1) the monomer DMAEMA (for #6: 500 equiv., for #7: 200 equiv.; final concentration: c(DMAEMA) = 5 mol/L) and HMTETA (1 equiv.) were dissolved in toluene and then degassed for 30 min. In parallel the macroinitiator (PBA, 1 equiv.) dissolved in toluene was degassed for 30 min. CuCl (1 equiv.) was added to the monomer solution and after 10 min of complex formation the macroinitiator was added via a syringe. Immediately, the flask was placed into an oil bath preheated at 50 °C for 150 min (for #6) or 270 min (for #7). The polymerization was quenched by THF, the solution was filtered through aluminum oxide and precipitated in cold hexane. The filtered polymer was dried overnight and characterized. To obtain a material with antimicrobial properties the polymer was firstly quaternized with 1-bromooctane in MeOH at 55 °C for 48 h under argon with a 3-fold excess of the quaternization agent compared to functional amino groups (c(1-bromooctane) = 1.8 mol/L), and secondly the remaining tertiary amino groups were quaternized with the less sterically hindered iodomethane in MeOH at room temperature for 20 h (c(MeI) = 1.8 mol/L) under argon. After each step, the solvent was removed, the residue was precipitated in hexane and the polymer was dried in oven overnight.

2.2.2. Synthesis of bulk coating polymer (PBMA)

The polymer which is used as bulk coating and reference material was PBMA synthesized via conventional free radical polymerization: A solution of BMA (c(BMA) = 1 mol/L) and AIBN (0.1 mol% with respect to BMA) in DMF was degassed for 30 min and the polymerization was conducted at 60 °C for 19 h. After removal of the solvent under reduced pressure, the residue was precipitated in MeOH and dried overnight to yield a polymer with M_n = 58 200 g/mol.

2.2.3. Preparation of functional coatings

95 wt% of PBMA and 5 wt% of the functional additive (#1–#7; Table 1) were dissolved in 3 vol% Milli-Q water, 38.8 vol% *n*-PrOH and 58.2 vol% EtOAc. The coatings were prepared in closed Petri dishes (inner diameter: 49 mm, A = 18.86 cm^2; Steriplan) by solvent evaporation from 5 mL polymer solution for 1 week. For captive bubble contact angle measurements and zeta potential measurements the coatings were also prepared inside those petri dishes but on commercially available glass cover slides (50 × 24 mm; Roth) which were firstly cleaned with KOH in *i*-PrOH, rinsed with Milli-Q water, dried in an argon stream, put into the Petri dish and then covered with the polymer solution. The coatings were peeled off the glass dishes and cut into strips, or the coated cover slides were cut out. The thickness of the resulting coatings without glass was measured with a micrometer (coolant proof micrometer, IP 65, 293–240, Mitutoyo Corporation); all values were in the range of 8–9 μm.

2.3. Measurements

2.3.1. Polymer analyses

Size exclusion chromatography (SEC) was performed in DMF containing 0.01 mol/L LiBr at 23 °C with an HPLC system based on a Waters 590 pump, a Shodex RI-71 detector and MZ SDplus columns

Table 1
Characteristics of functional additives.

	M_n (PBA) (g/mol)[a]	PDI	M_n (PBA-*b*–PNIPAAm) (g/mol)	PDI	% PNIPAAm via ^{1}H NMR
PBA-*b*–PNIPAAm					
#1	15 000	1.56	49 800	1.16	57
#2	15 000	1.56	37 800	1.22	29
#3	7500	1.62	37 500	1.18	57
#4	8300	1.10	36 000	1.21	62
#5	3900	1.14	25 000	1.13	51

	M_n (PBA) (g/mol)	PDI	M_n (PBA-*b*–PDMAEMAq) (g/mol)	PDI	% PDMAEMA via ^{1}H NMR	% Octyl groups	% Methyl groups
PBA-*b*–PDMAEMAq							
#6	7100	1.06	34 500	1.31	63	82	18
#7	8300	1.10	57 400	1.42	75	78	22

[a] For the synthesis of PBA of block copolymers #1, #2 #3, and #5 Me_6TREN and CuCl as catalyst were used and resulted in a less controlled ATRP (for exact conditions and related kinetic investigations see Ref. [25]).

effective in the 50–5000, 1000–70000 and 100–>2000000 molecular weight ranges (all numbers in g/mol). For calibration poly(methyl methacrylate) (PMMA) standards were used. ^{1}H NMR spectra were recorded in $CDCl_3$ or, for the cationic polymers, in methanol-d_4 with a Bruker DMX-300 (300 MHz) at 25 °C.

2.3.2. ATR-IR spectroscopy

The coating's surface chemistry was analyzed by attenuated total reflection (ATR) Fourier transform infrared (FTIR) spectroscopy, using the instrument Varian 3100 Excalibur series (equipped with an MCT detector, GE crystal, 60°). For determination of the amount of PNIPAAm accumulated at one side of the coating the ratio of the height of the amide band of PNIPAAm at 1542 cm^{-1} and of the ester band of PB(M)A at 1723 cm^{-1} was calculated.

2.3.3. Contact angle measurements

Contact angles (CA) were determined using an optical measurement system (OCA 15 Plus, Dataphysics GmbH, Filderstadt, Germany). Static and dynamic CA data were measured with the sessile drop method. Using a 0.5 mL Hamilton syringe with a straight needle with an inner diameter of 0.26 mm a drop of 5 μL Milli-Q water was placed onto the surface and the static CA was measured. With the needle remaining inside the drop advancing (CA_{adv}) and receding (CA_{rec}) contact angles were measured by increasing and decreasing the water volume of the drop with a rate of 0.5 μL/s, respectively. Static CA were also measured using the captive bubble method on coated cover slides: an air bubble of 5 μL was injected from the same syringe but with a bent stainless steel needle onto the inverted sample surface immersed into Milli-Q water. All samples were firstly equilibrated for at least 1 min in Milli-Q water and contact angles were measured at 1 min after deposition of the bubble onto the surface. For temperature dependent static contact angles the temperature of the Milli-Q water was raised to 43 ± 1.1 °C; in all other cases, temperature was 20 ± 1.0 °C. For both methods the Dataphysics software was used for estimation of the contact angle values. For each value at least three drops or bubbles were measured for one sample and data for each surface were averaged over values for three independently prepared samples. The data presented is given as a mean value and standard deviation. The contact angle hysteresis is calculated from the advancing and receding values as follows:

$$\Delta CA = CA_{adv} - CA_{rec} \quad (1)$$

2.3.4. Zeta potential

The surface charge was investigated by a streaming potential measurement. Experiments were carried out in a flat-sheet tangential flow module [26]. Two coated glass slides were placed above and below the spacer, with both the air sides of the coating facing the flow channel. The system was equilibrated for at least 45 min in a 0.001 mol/L KCl solution as electrolyte pumped by a variable-speed pump drive from Vancouver, USA (model 120-00, Series 1552085). Pressure was measured using a pressure transducer by Setra Systems, USA (model 280 E). Streaming potentials were measured in the range of pH of 4–10 at a temperature of 25 ± 1 °C, increasing the pressure step-wise (in the range of 65–100 kPa) at each pH. The pH was adjusted by addition of KOH and HCl solutions and equilibration for at least 20 min and measured using a pH-meter by Radiometer, Danmark (PHM 62 Standard). The conductivity was recorded with a WTW microprocessor conductivity meter LF 535. A digital voltmeter by Voltcraft, Germany, was used for measuring the streaming potential. The zeta potential ζ was determined using the Helmholtz–Smoluchowski equation:

$$\zeta = \frac{\kappa\eta}{\varepsilon_0\varepsilon}\frac{\Delta E}{\Delta P} \quad (2)$$

where ΔE is the streaming potential, ΔP the hydrodynamic pressure difference, η the viscosity, ε the dielectric constant of the solvent, ε_0 the permittivity of the vacuum and κ the conductivity of the solution.

2.3.5. Determination of ammonium groups

The accessible quaternary ammonium groups of the various coatings were measured by a colorimetric method based on fluorescent complexation and UV/Vis spectroscopy, as described by Tiller et al. [27]. A functional coating (punched to 1.54 cm^2) was immersed in a 1 wt% solution of fluorescein (Na salt) in Milli-Q water for 10 min, rinsed with Milli-Q water three times, placed in 5 mL of 0.1 wt% cetyltrimethylammonium chloride in Milli-Q water and shaken for 20 min to desorb the dye. The absorbance of the resulting aqueous solution was measured at 501 nm after adding 10 vol% of an aqueous phosphate buffer, pH 8.0. The concentration of the fluorescein dye was calculated; the value of 44 mM^{-1} cm^{-1} for the absorbance coefficient had been independently determined.

2.4. Microbiological experiments

2.4.1. Preparation of cell suspensions

S. aureus ATCC 25923 was grown at 37 °C overnight on a tryptic soy agar (15 g/L peptone from casein, 5 g/L peptone from soybean, 5 g/L NaCl and 15 g/L agar, autoclaved for 20 min). A colony of the culture was suspended in phosphate-buffered saline (PBS; 8.2 g/L NaCl and 1.2 g/L $NaH_2PO_4 \cdot H_2O$, pH adjusted to pH 7 with 1 M NaOH, autoclaved for 20 min) to yield approximately 1.5×10^9 cells/mL. 1 mL of this suspension was used to inoculate 20 mL of tryptic soy broth (17 g/L peptone from casein, 3 g/L peptone from soybean, 2.5 g/L D(+) glucose, 5 g/L NaCl, 2.5 g/L K_2HPO_4, autoclaved for 20 min) in a 100 mL sterile Erlenmeyer flask. The culture was incubated in a shaking water bath at 180 rpm at 37 °C for 18 h. The bacterial cells were harvested by centrifugation at 5000×*g* for 10 min at 4 °C (Sorvall RC 26 Plus Superspeed Centrifuge), washed twice with 20 mL PBS, resuspended in 20 mL PBS, and the cell suspension was diluted with PBS to the desired final cell concentration.

2.4.2. Microscopic determination of cell viability by fluorescent labeling

Petri dishes coated with PBMA and a cationic additive (#6 or #7) or pure PBMA were filled with 6 mL of a *Staphylococcus aureus* suspension (10^7 cells/mL) and incubated statically at room temperature for 30 min, 1 h and 2 h. The suspension was removed and the coatings were air-dried. A cell staining solution was freshly prepared by adding 1.5 μL SYTO 9 and 1.5 μL propidium iodide of the LIVE/DEAD *Bac*Light Bactericidal Viability Kit to 997 μL PBS. 100 μL of the mixture were added to the surface of the coated Petri dish. After incubation in the dark for 15 min at room temperature, the solution was removed and the coatings were air-dried again. One drop of antifading reagent (Citifluor AF2) was placed on the stained area and was covered by a glass coverslip. After adding a drop of immersion oil on the coverslip, enumeration of the bacterial cells was performed at 1000× magnification using an epifluorescence microscope (Laborlux S, Leica). The data presented has been confirmed in two independently repeated experiments.

2.4.3. Cultural determination of bactericidal efficiency

Petri dishes coated with PBMA and a cationic additive (#6 or #7) or pure PBMA were filled with 6 mL of a *S. aureus* suspension (5×10^3 cells/mL) and incubated statically at room temperature for

30 min, 1 h and 2 h. Coated Petri dishes treated in the same way in parallel but with PBS instead of cell suspension were used as control. After removal of the cell suspension the coatings were rinsed with 6 mL PBS, dried and immediately covered with tryptic soy agar heated at 45 °C. The agar medium was allowed to solidify at room temperature. After incubation of the petri dishes at 37 °C overnight, the bacterial colonies were counted and the results were calculated as colony-forming units (cfu) per cm^2. The bactericidal effect was calculated as

$$\text{bactericidal effect} = \frac{\text{cfu}_{\text{PBMA+additive}} \times 100}{\text{cfu}_{\text{PBMA}}} \quad (3)$$

The values presented are average values from three independently repeated experiments with two coatings analyzed at each time.

3. Results and discussion

3.1. Temperature responsive coatings with PBA-b-PNIPAAm as additive

3.1.1. Determination of surface enrichment

PBMA coatings with PBA-*b*-PNIPAAm as additive were prepared by selective solvent evaporation in Petri dishes. The used solvent mixture composition (3 vol% water, 38.8 vol% *n*-PrOH and 58.2 vol% EtOAc) had been identified in preliminary experiments with sufficient solubilities of PBMA and PBA-*b*-PNIPAAm as one criterion. The particular influence of the small fraction of water will be presented and discussed in Section 3.1.2. For investigation of the surface enrichment of the additive at one interface, the obtained films were peeled off the glass and cut. In the following the air interface will be called the "air side" of the coating and the interface facing the glass of the Petri dish will be referred to as the "glass side".

Firstly, the influence of molecular weight and block ratio of the functional additive on the surface enrichment of the coating was investigated. All coatings were prepared with 5 w% of the block copolymer except the coating containing additive #2. This additive did not fully dissolve in the solvent mixture. Pure PBMA is soluble in this mixture and as all the other additives, especially additive #1 with the same PBA block but a longer PNIPAAm chain, were also soluble, the small PNIPAAm block in polymer #2 (29% PNIPAAm) seems to be responsible for the reduced solubility. Apparently, the hydrogen bonding and polar binding strengths of the solvent mixture had been slightly too high for this PBA-rich copolymer (cf. Fig. 2). Therefore, only the supernatant saturated solution of polymer composition #2 was used for the formation of the polymer film.

The functional groups at the air and the glass interface were investigated using ATR-IR spectroscopy. This method is surface selective, but analyzes about the top 1 μm of the polymer surface [3]. A comparison of the band ratios of the amide of the PNIPAAm and the ester of the PBA and PBMA at the air and the glass side is shown in Fig. 3.

The results obtained by ATR-IR spectroscopy show that enrichment of PNIPAAm at the air surface of the coating was obtained for all additives as the ratios for the air sides are all higher than for the glass sides. The relative amount of PNIPAAm found at the air interface correlates quite well with the absolute PNIPAAm content in a block copolymer: for the additives #1 and #4 with the highest molecular weight of PNIPAAm, calculated from total molecular weight and percentage of PNIPAAm, the highest ratios were observed; for the additives #2 and #5 with the lowest molecular weight of PNIPAAm the lowest ratios were found. This fact indicates that the driving force for air surface enrichment of the additive is

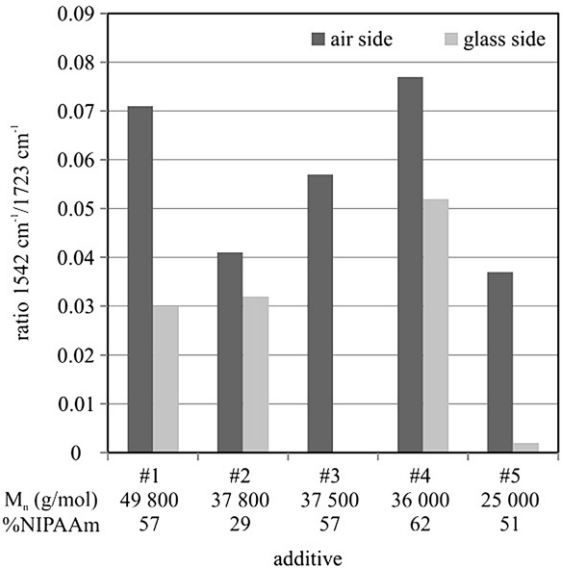

Fig. 3. Results of ATR-IR spectroscopy: the amount of PNIPAAm enriched either on the air or the glass side of the coating was determined as the ratio of the height of the amide band of PNIPAAm at 1542 cm^{-1} and of the ester band of PB(M)A at 1723 cm^{-1}; M_n was obtained by SEC calibrated with PMMA, and the percentage of NIPAAm of the block copolymer was analyzed by ^1H NMR (cf. Table 1).

the solubility of the PNIPAAm in the residual solvents water and *n*-PrOH. Although additive #1 with the highest molecular weight is supposed to have the lowest rate of diffusion during the film forming process, the solution enthalpy seems to be the dominant factor for the migration and a high amount of PNIPAAm at the air side can be found. Also, solidification of the polymer film is apparently slow enough to allow thermodynamic control.

Nevertheless, for the additives #1, #2 and #4 amide groups could be also identified at the glass side of the coating. This means that migration of the additive exclusively to the air side of the coating did not occur. Perhaps due to the hydrophilic character of glass, presumably also containing some adsorbed water, an enrichment of hydrophilic PNIPAAm at the glass interface can be observed, too. This theory is further supported by the results of a control experiment on hydrophobically silanized glass. Under these conditions, surface enrichment of additive #4 at the air interface could be enhanced (cf. Table S1, Supplementary content). However, as the relative amounts of PNIPAAm found at the glass side of the coating do not correlate with the total molecular weights of PNIPAAm (as discussed above) and were always lower than at the air side, a selective migration to the interfaces is more probable than a random distribution of the additive in the entire coating volume. This assumption is strongly supported by the fact that additives #3 and #5 did accumulate only at the air side of the coating as nearly no amide groups could be detected at the glass side. It can be concluded that for a certain relatively narrow range of molecular weight and block ratio (with #3 and #5 as examples) a highly selective migration of the additive to the air interface of the coating can be obtained.

For further investigations static contact angles of both, the air and the glass side were measured. The results of this technique refer to a much thinner layer (outer ~5 Å of the coating) than those obtained by ATR-IR spectroscopy [3]. Fig. 4 shows that the addition of PBA-*b*-PNIPAAm to PBMA changed the contact angle of the air side from 92.1 ± 0.5° for pure PBMA to a value around 65° for all additive-containing coatings. This means that at the outer surface properties of the coatings in terms of wettability were changed in the same way for all additives (note that additive #2 was not fully

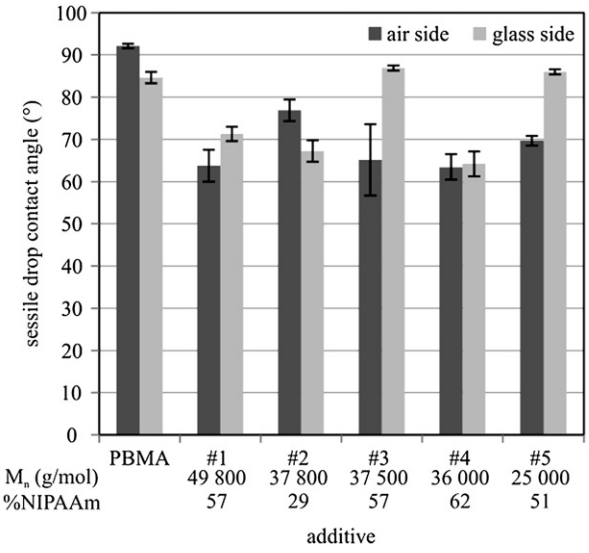

Fig. 4. Contact angle of the coating's air and glass sides for pure PBMA and for the films with different temperature responsive additives (cf. Table 1).

dissolved in the casting solution, so that the resulting coating contained a lower percentage of additive).

This observation does not match with the results of the ATR-IR spectroscopy. Reasons could be the difference in the sampling depth of the two methods or the fact that the collapsed PNIPAAm chains in the dry state cover the outer surface of the coating in a way that no differences in static contact angle for different additives can be measured. Therefore, dynamic contact angle measurements were additionally performed. From the hysteresis data in Table 2 it can be concluded that also the homogeneity and roughness for the air sides of all coatings were nearly the same (the largest deviation was again observed for additive #2 present in lower overall content; cf. above). However, the hysteresis differed very much from that obtained for pure PBMA. These results were also supported by AFM images in which a clear difference between the air surface of pure PBMA and a coating with additive #3 is observed (cf. Fig. S1, Supplementary content).

When looking at the static and dynamic contact angles of the glass sides, it can be deduced that the hydrophilic glass of the Petri dishes influenced the surface properties of pure PBMA as the contact angle and the hysteresis were smaller at the glass side of the coating (cf. Fig. 4 and Table 2). The glass sides of the coatings with additives #1, #2 and #4 showed even more hydrophilic properties compared to the glass side of pure PBMA. This means, as already observed by ATR-IR spectroscopy, for these additives the migration to the air interface is not selective and some enrichment at the glass side of the coating can also be observed. For additives #3 and #5 highly selective enrichment at the air interface had been found via ATR-IR spectroscopy. These results are strongly confirmed by the static contact angle values and the hysteresis for the glass sides of both coatings, because both are essentially identical to the values for the glass side of pure PBMA. In summary, by combining the results of both analytical methods, highly selective surface enrichment of the block copolymer additive at the air interface of the coating can be obtained for block copolymers with a nearly 1:1 block ratio of anchor block and functional block, but only if the molecular weight is not to high (<37 500 g/mol).

3.1.2. Determination of temperature responsive properties due to surface segregation

The main aim of this work had been to prepare coatings, composed of a bulk material and a functional surface layer, with functionalities that would not be accessible for the bulk material alone. Surfaces that are able to change their properties with respect to wettability and swelling upon an external stimulus like temperature have been shown to be a useful tool for applications such as tissue engineering [28] or biofilm release [15–18,29]. The temperature dependent properties of the coatings with PBA-*b*-PNIPAAm as additive were investigated measuring captive bubble contact angles at a temperature below the LCST of PNIPAAm and above (Fig. 5). Taking a closer look at the contact angle values at 20 °C for the coatings with the different additives, this method allows a more detailed interpretation than the sessile drop method (cf. Fig. 4). It can be seen that for the highest molecular weight block copolymer (#1) the lowest captive bubble contact angle and thus the most hydrophilic surface in equilibrium with water was observed. This might be due to the long PNIPAAm chains which swell in water and thereby shield the hydrophobic influence of the underlying PBMA layer. Further, with the lowest molecular weight additive (#5) a more hydrophilic surface could be obtained than for the other additives (#2–#4). As the PNIPAAm chains in additive #5 are very short, a more dense surface coverage with this additive should cause the lower contact angle. From the other results (cf. 3.1.1) it had been deduced that the entire amount of this additive is located in the air surface region of the coating. That the contact angles under water were higher for coatings with additive #3, with analogous highly selective accumulation at the air interface (cf. 3.1.1), could indicate that with the larger PNIPAAm coils "grafted" to the surface, a less efficient screening of the underlying hydrophobic PBMA had been achieved.

The comparison of the contact angles at 20 °C and 43 °C reveals that all surfaces with additives become more hydrophobic at 43 °C (cf. Fig. 5). This property is not related to the bulk polymer PBMA as this shows lower contact angles at 43 °C which is due to the temperature dependence of the surface tension of water. Even though exclusive enrichment at the air surface had not been achieved with all additives, all coatings exhibited temperature responsive properties. Consequently, the enrichment of the additives at the air interface of the coating is followed by a segregation which leads to conformationally flexible PNIPAAm chains (cf. Fig. 1b). In water, these chains are able to react freely to environmental conditions without hindrance of the bulk coating. It is remarkable that without the addition of 3% of water during the film

Table 2
Advancing contact angle and contact angle hysteresis of the air and glass sides of pure PBMA and coatings containing different temperature responsive and cationic additives.

	M_n (g/mol)	% Active block	CA_{adv} air side (°)	CA_{adv} glass side (°)	ΔCA air side (°)	ΔCA glass side (°)
PBMA			90.5 ± 0.9	86.2 ± 2.2	11.7 ± 0.4	8.3 ± 2.3
#1	49 800	57	57.0 ± 4.8	65.3 ± 2.6	29.9 ± 2.1	31.9 ± 13.3
#2	37 800	29	71.1 ± 5.2	70.3 ± 2.5	23.4 ± 7.4	21.4 ± 2.8
#3	37 500	57	61.7 ± 9.8	85.4 ± 2.7	28.8 ± 9.1	10.4 ± 1.3
#4	36 000	62	59.8 ± 3.1	61.5 ± 3.8	28.1 ± 3.7	21.6 ± 3.0
#5	25 000	51	79.3 ± 1.4	87.9 ± 2.0	32.6 ± 1.4	12.8 ± 1.7
#6	34 500	63	90.5 ± 2.1	88.0 ± 3.3	28.6 ± 2.7	13.6 ± 3.9
#7	57 400	75	86.4 ± 1.8	85.6 ± 2.6	16.4 ± 2.2	12.4 ± 1.4

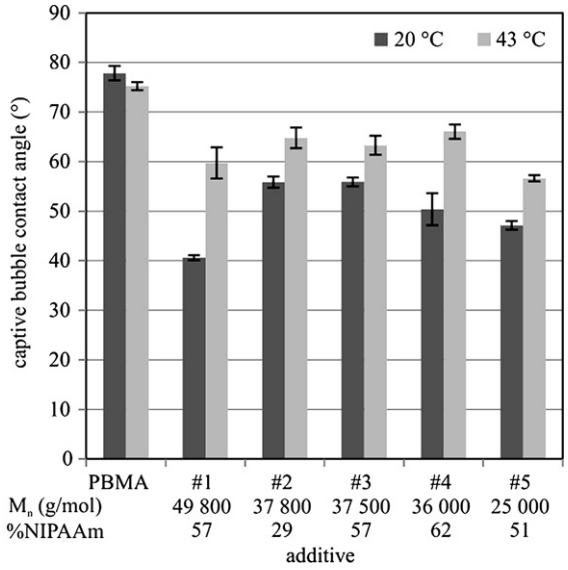

Fig. 5. Results for contact angle measurements via the captive bubble method at temperatures below (20 °C) and above (43 °C) the LCST of PNIPAAm (32 °C) of the coating's air side for pure PBMA and PBMA with different temperature responsive additives (cf. Table 1).

preparation process, no temperature responsiveness was observed for any additive although surface enrichment had been proven similar to the results above (cf. 3.1.1). Therefore, without traces of water, the driving force for PNIPAAm to segregate at the air surface is reduced and leads to a surface layer in which PNIPAAm is accumulated but is still strongly entangled in the bulk polymer. Those PNIPAAm chains are not able to respond to the temperature changes in terms of significant swelling/deswelling transition. In conclusion, a small amount of water induces surface segregation of the additive and thereby is responsible for the temperature responsive functionality of the resulting coatings.

The absolute values of contact angles at temperatures below and above LCST, i.e. the degree of switchability, for PNIPAAm surfaces are already inconsistent in literature [30]. The influences of the preparation of the surface and of the analysis technique on the observed degree of switchability are too pronounced to allow a conclusive quantitative comparison with the data obtained in this work. Nevertheless, applying the same techniques for all coatings in this work is a sound basis for a valid comparison of the different additives. The difference between the contact angles at 20 °C and 43 °C in this study was the highest for additive #1 and #4 (cf. Fig. 5). These two block copolymers have the highest molecular weight PNIPAAm chains among all additives. This may indicate that the degree of switchability depends on the length of freely mobile chains at a surface, a fact that is already discussed in literature [31]. On the other hand, the observation may be also due to the relatively low surface coverage of the respective coatings. As indicated above, contact angle measurements are only sensitive to the very outer layer of the surface region. Swollen long PNIPAAm chains at low surface coverage may be able to shield the underlying PBMA film, but once these chains collapse at temperatures above the LCST, they form a loose pattern of compact coils which is no longer able to effectively shield the PBMA completely. For the additives #3 and #5 a lower difference between the contact angles at different temperatures is observed. Due to the lower molecular weight (compared to #1), the resulting coatings have a higher surface coverage with PNIPAAm, as already discussed above, and the change of surface coverage with temperature becomes smaller.

In summary, the influence of molecular weight of the additives and the block ratio on surface enrichment and segregation has been shown. Furthermore, the functionality, i.e., temperature responsiveness, has been proven for all additives. Based on these results the optimal additive was chosen to be block copolymer #3. Additive #3 and #5 were the only block copolymers that fully enrich at the air interface of the coating which leads to an effectively lower amount of additive needed for high surface coverage. Furthermore, additive #3 is anticipated to have a lower tendency to leach out from the surface as it has a higher molecular weight than additive #5 [4].

3.1.3. Reversibility of the switching effect and long term stability of the surface functionalization

As described above block copolymer #3 was chosen as optimal additive for surface segregation applying the coating preparation procedure developed in this study. This coating was tested for its reversible switching effect upon temperature changes. As can be concluded from Fig. 6, the PNIPAAm chains undergo the conformational changes around the LCST at least over ten consecutive cycles. The degree of switchability deduced from the difference in contact angle at 20 °C and 43 °C increased in the second switching cycle and then remained almost constant. Additionally, the coatings were stored in water for 6 days and the contact angles and temperature responsiveness was measured once again. Fig. 6 shows that no changes in the contact angle at 20 °C can be detected; hence no block copolymer additive had leached out. Furthermore, the coating also fully maintained its functionality in terms of switchability as the contact angles at 43 °C remained constant, too.

3.2. Bactericidal coatings with PBA-b-PDMAEMAq as additive

3.2.1. Characterization of surface properties

Encouraged by the results obtained for temperature responsive block copolymers as additives, the same approach was also applied to the bactericidal polymers PBA-*b*-PDMAEMAq. Surfaces that kill bacteria upon contact based on hydrophobically quaternized nitrogen compounds are known in literature, e.g., prepared by surface initiated polymerizations [32], by using the "grafting to" approach of block copolymers [33], by copolymerization of the polycation with a hydrophobic side chain that allows a one-step, painting-like procedure [34], by applying the layer by layer technique [35] or by surface modification of polyurethane with soft blocks [36], but still their mechanism of operation is not clear. Either the penetration of the hydrophobic alkyl chain into the bacterial cytoplasmic membrane [27] or the substitution of the structurally critical divalent cations such as Ca^{2+} or Mg^{2+} by the polycation [37] may lead to a change of membrane integrity and cause cell death. In order to distinguish between both mechanisms, the same block copolymers were also quaternized only with iodomethane instead of firstly with bromooctane and secondly with iodomethane (cf. 2.2.1). Unfortunately, the block copolymers with only methyl groups were not soluble under the conditions applied in this approach to prepare functional coatings. Therefore, no further investigations about the killing mechanisms in dependency of the alkyl chain length can be presented here because the block copolymers #6 and #7 had been quaternized with a combination of about 80% long octyl chains and 20% short methyl groups (cf. Table 1).

Firstly, the same characterization methods as described above (cf. 3.1.1) for determination of the influence of molecular weight on the surface enrichment were applied. Unfortunately, neither characteristic IR bands of the additive which are distinguishable to the PBMA bands nor significant changes in contact angles upon additive addition to PBMA could be detected. Only the differences in the contact angle hysteresis for the air and glass sides of both coatings indicate a surface enrichment/segregation as discussed above (cf.

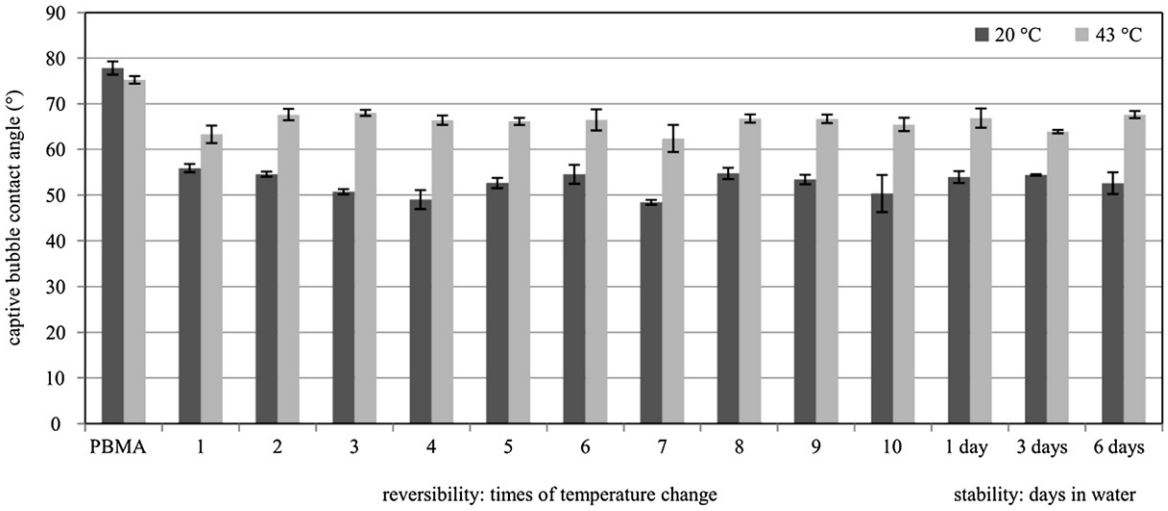

Fig. 6. Reversibility of the switching effect and long term stability of the PBMA-based coating with additive #3 (M_n = 37 500 g/mol by SEC and 57% PNIPAAm by ^{1}H NMR; cf. Table 1).

Table 2). Therefore, other techniques such as the determination of the cationic groups at the surface or zeta potential measurement were used.

The accessible cationic groups were determined using an anionic dye. For surfaces that had been prepared with additive #6 6.59 ± 0.89 nmol/cm^2 cationic groups could be detected. In contrast to this, for the higher molecular weight additive #7 with a higher block ratio and thus more cationic groups per additive molecule only 2.32 ± 0.41 nmol/cm^2 could be found. Assuming that for both additives the same surface enrichment had been achieved, this result indicates that the high molecular weight additive #7 does not fully segregate at the air side of the coating but is still partly entangled in the bulk polymer. It cannot be concluded whether coatings with additive #6 are fully surface segregated but significantly more cationic groups are accessible at the surfaces. For a dense two-dimensional layer of ammonium cations having one octyl group a charge density of 0.05 nmol/cm^2 was estimated. Taking this value into account, for both additives #6 and #7 a pronounced three-dimensional structure of the layer with cationic groups is highly probable. This means that the functional block of the additive is conformationally free immobilized in a functional layer at the surface (cf. Fig. 1b). For a bactericidal effect via the membrane disruption mechanism, the functional block has to be sufficiently flexible to be able to penetrate the bacterial cell membranes. For the surfaces with both additives this precondition is fulfilled. A minimum wet layer thickness of a polymer layer of 75 nm had been postulated in order to effectively penetrate the cytoplasmic membrane and kill the cells; this means that at least a M_w of 75 000 g/mol for the cationic polymer chain would be required to be able to penetrate a cell [38]. Both additives in this study have a smaller molecular weight. Regarding the killing mechanism via release of the structurally essential divalent cations by polycation substitution, it has been suggested that a surface with greater than 5 × 10^{15} charges/cm^2 will be able to kill at least a monolayer of *E. coli* cells [38]. The coatings with additive #6 have a sufficiently high charge density (4 × 10^{15} charges/cm^2), whereas coatings with additive #7 (1 × 10^{15} charges/cm^2) should show a lower killing potential.

Additionally, the outer surface of the coatings was characterized by zeta potential measurements. Once again, the two techniques analyze different depths of the coating: while the anionic dye binds to every cation which is accessible in a three-dimensional water-swollen polymer layer, the zeta potential results from the very outer surface cations of that layer which are accessible to the shear by tangential convective flow. In Fig. 7 the comparison of the zeta potentials of pure PBMA and coatings with additives #6 or #7 in dependence of the pH is shown.

The pure PBMA surface showed a zeta potential curve which is typical for a non ionic surface; surface charge is dominated by ion adsorption from the electrolyte solution [39]. In contrast, air sides of both coatings with block copolymer additives exhibited strong cationic properties for a pH range from ~4 to ~10. This indicates that both cationic additives dominate the air side surface properties of the coating. The absolute zeta potential was higher for coatings with additive #6 which is qualitatively well in line with the results for cation group density (cf. above). Correlating all data with the postulations made in literature with regard to the cation substitution mechanism, the coatings with additive #6 are believed to exhibit a higher killing efficiency against bacteria. In contrast, coatings with additive #7 should kill bacteria more efficiently by the penetration mechanism due to their longer flexible cationic chains.

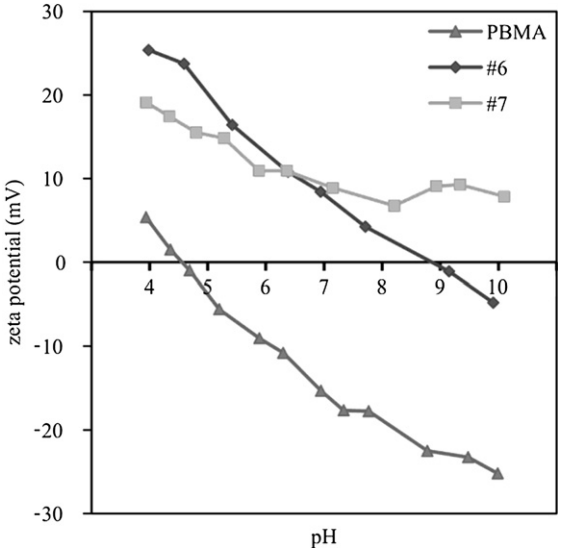

Fig. 7. Dependency of the zeta potential on pH for the air side of pure PBMA coating and coatings with additives #6 (M_n = 34 500 g/mol by SEC, 63% PDMAEMAq via ^{1}H NMR) or #7 (M_n = 57 400 g/mol by SEC, 75% PDMAEMAq via ^{1}H NMR; cf. Table 1).

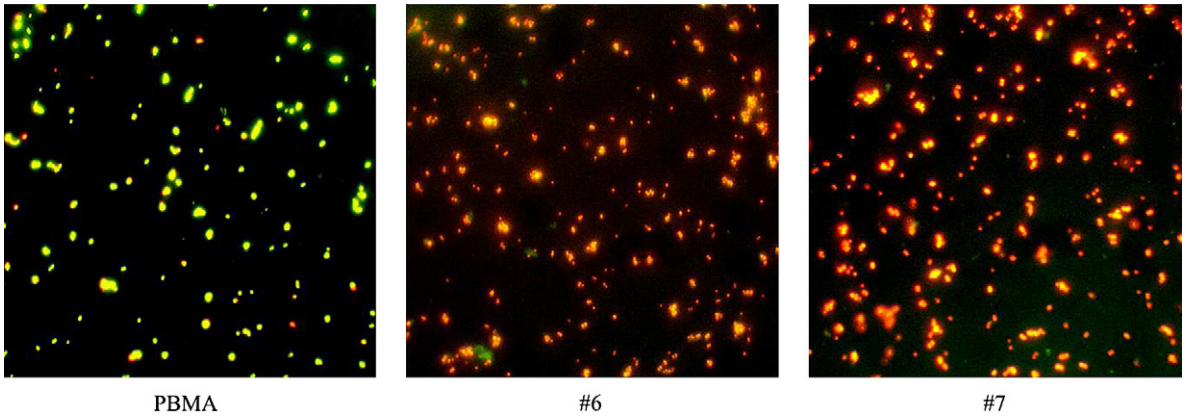

Fig. 8. Fluorescence microscopy images (1000× magnification) of *S. aureus* after 2 h contact at room temperature with a pure PBMA coating, a coating with additive #6 (M_n = 34 500 g/mol by SEC, 63% PDMAEMAq via ^{1}H NMR) and a coating with additive #7 (M_n = 57 400 g/mol by SEC, 75% PDMAEMAq via ^{1}H NMR; cf. Table 1); green and red cells are clearly distinguishable in each case.

3.2.2. Bactericidal effect

Another method to determine surface segregation of PBA-*b*-PDMAEMAq in PBMA is the evaluation of the killing efficiency of the coating against bacterial cells. In the present study, the gram-positive bacterium *Staphylococcus aureus* was employed to investigate the bactericidal effect of the coatings. This organism has previously been shown to be suitable for demonstrating the damage of cell membranes and the killing of cells (loss of culturability) upon contact with bactericidal surfaces [34,40].

In a first series of experiments, *S. aureus* cells were contacted for 30 min, 1 h and 2 h with coatings with and without cationic additive. The adhering cells were visualized microscopically after fluorescent staining of the bacteria directly on the surfaces (Fig. 8), using the two DNA-binding fluorescent dyes SYTO 9 and propidium iodide (cf. 2.4.2). SYTO 9 generally labels all bacteria in a population with both intact and damaged membranes, while propidium iodide penetrates only bacteria with damaged cell membranes [41]. Using a mixture of SYTO 9 and propidium iodide, bacteria with intact membranes fluorescence bright green, whereas in bacteria with damaged membranes, propidium iodide abolishes the green fluorescence of SYTO 9 by displacing this dye from complexes with DNA and causes these cells to fluoresce red. Thus, using a combination of SYTO 9 and propidium iodide allows distinguishing between live and damaged/dead bacterial cells. The density of surface attached bacteria was similar on all three surfaces and increased with increasing time of incubation: for 30 min—8.6×10^5 cells/cm^2, for 1 h—1.2×10^6 cells/cm^2 and for 2 h—3.6×10^6 cells/cm^2 (cf. Fig. 8 for 2 h) could be detected. However, the ratio of green to red fluorescent cells differed, depending on the type of coating. Pure PBMA exhibited no killing effect whereas both coatings with PBA-*b*-PDMAEMAq as additive had a significant impact on the cell membrane integrity.

By counting the ratio of intact (green) to damaged (red) cells the killing efficiency of a coating with additive #6 increased from 77.7 ± 9.8% for 30 min of contact to 90.1 ± 2.7% for 1 h and to 95.6 ± 1.9 %for 2 h (the percentage of damaged cells on the PBMA surface was 10.2 ± 3.8%). The corresponding values for coatings with additive #7 did not depend on time (30 min: 97.7 ± 2.2%; 1 h: 95.1 ± 1.7% and 2 h: 95.9 ± 2.8%) and were comparable to that of coating with additive #6 at 2 h. The functional PDMAEMAq blocks of the additives have to be segregated at the surface to some extend for exhibiting these properties. As there was a distinct difference in the surface chemistry/architecture between coatings with additives #6 and #7 (cf. 3.2.1), the difference in the time dependent bactericidal effect against *S. aureus* could be related, but this difference leveled off for incubation times of 2 h.

In a second set of experiments, the bactericidal effect was investigated by the determination of the influence of the coating on the culturability of *S. aureus*. The bacteria were allowed to adhere to the coatings for 30 min, 1 h and 2 h; subsequently, the surfaces were rinsed with buffer and overlaid with tryptic soy agar. After incubation at 37 °C overnight the colonies were counted and the colony-forming units/cm^2 were calculated. As can be seen in Fig. 9, there was a time dependent growth-inhibiting effect for both coatings, but the efficiency was always more pronounced for the higher molecular weight additive #7 than for #6. After 30 min of bacterial adhesion there was the lowest killing effect. Upon increase of adhesion time to 2 h more and more cells were attached to the surface as can be seen from the live/dead staining, but also a higher percentage of cells was killed upon contact with the surface (cf. above). For coatings with the smaller additive #6 91.7% of *S. aureus* were not able to form colonies after 2 h of adhesion, whereas with the higher molecular weight additive #7 a 99.2% decrease of culturability was observed (cf. Fig. 9).

In parallel to the observations made by staining with the live/dead kit, the analysis of the bactericidal effect based on the

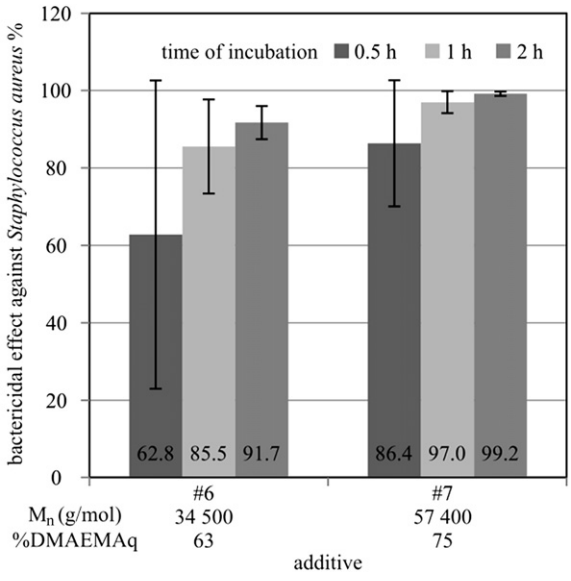

Fig. 9. Bactericidal effect based on colony-forming units (cfu) determined on tryptic soy agar layered on coatings with PBA-*b*-PDMAEMAq (cf. Table 1) as additive in comparison to PBMA; the percentages of the bactericidal effect were calculated relative to the cfu on pure PBMA (n = 3; see 2.4.3).

determination of colony counts revealed that the two additives with different molecular weights exhibited different properties. Although a higher charge density and zeta potential had been found for coatings with additive #6, surface segregated coatings with additive #7 exhibited a higher potential to disrupt the cell membranes of *S. aureus*. Comparing the two microbiological methods it should be considered that cells stained as red and thereby supposed to be damaged, are not necessarily killed but may be still able to form colonies. Nevertheless, in this study a correlation between results of both series had been found with respect to the activities of the functional additive. Looking at the differences of the coatings with different additives, these results do not correlate with the estimations made in literature for a cation substitution mechanism (cf. 3.2.1). The results of our study indicate that the higher molecular weight additive with a lower charge density is more effective against *S. aureus* and thereby suggest that the penetration of the cytoplasmic membrane by the alkyl chains is the dominating mechanism (there is only some discrepancy to estimations in literature with respect to the minimum chain length; cf. 3.2.1). Similar observations of an increase of the killing efficiency by increase of the molecular weight of the bactericidal polymer have already been made which led to the theory that the alkyl chain penetration is the mechanism of action of these polymers [34].

Regardless of the detailed mechanistic implications, the results of this study clearly show that the addition of PBA-*b*-PDMAEMAq to PBMA along with film formation via sequential evaporation of selective solvents results in functional surface segregated coatings that exhibit bactericidal properties.

4. Conclusion

Surface segregated coatings with either temperature responsive or bactericidal properties were prepared via sequential solvent evaporation. The advantage of this approach is that only a small amount of block copolymer (5 wt%) is needed to obtain a functional coating. Additionally, due to the additive's architecture with an anchor block compatible to the bulk polymer, the functionalization should have long term stable in aqueous media. The pre-estimation of the selective solubility and sequential evaporation based on the Hansen solubility parameters and vapor pressures, respectively, was found to work very well for an optimal molecular weight and block ratio of the additive: using PBA-*b*-PNIPAAm as additive a molecular weight of 37 500 g/mol with 57% of PNIPAAm was found to fully surface segregate only at the air interface of the coating. Remarkably, a small fraction of water in the solvent mixture had been crucial to obtain the full functionality. This functionalization of PBMA was successful as the coatings exhibited fully reversible temperature dependent wetting properties which were stable for at least 6 days in water. Furthermore, the addition of PBA-*b*-PDMAEMAq to PBMA resulted in coatings with cationic properties on the air side detectable via dye staining and zeta potential measurements. The killing efficiency of the coating depended on the molecular weight of the additive/functional block: for an additive with 57 400 g/mol and 75% of the active cationic block a bactericidal effect of 99.2% after 2 h of adhesion of *S. aureus* was determined via cfu measurements, relative to the unmodified bulk polymer. That the two different types of additive could be processed to functional films under identical conditions implies that coatings with mixed functionality can be obtained by using mixtures of the additives. All results are very promising for alternative preparations of anti-fouling and anti-biofouling surfaces, but they have also implications for other applications.

Overall, this straight forward approach of sequential evaporation of selective solvents is believed have broader impact to prepare functional coatings from polymer blends with accessible functional groups and thereby of materials with tailored surfaces. The incorporation of an additive in the surface layer of a material has great impact on its performance. The block copolymer architecture of the additive allows adaptation of each individual block for the needs of the material. The anchor block is chosen to be chemically similar to the bulk material and the functional block can be tailored for the application. As an example, it has already been shown that the segregation of an amphiphilic block copolymer additive in the pore surface layer of a polyethersulfone microfiltration membrane has a great impact not only on the surface properties but also on the filtration and separation performance [42]. Further investigations regarding the feasibility of that approach for preparation of functional filtration membranes using the additives used in this work are underway.

Acknowledgments

The authors thank Young Lim, student at Southern Methodist University, Dallas, USA, and supported during his stay in Essen via the RISE program of the German Academic Exchange Foundation (DAAD) for his assistance in polymer synthesis, Dieter Jacobi (Technische Chemie at Universität Duisburg-Essen) for the SEC analysis, and Prof. Dr. Hans-Curt Flemming (Biofilm Centre, Universität Duisburg-Essen) for stimulating discussions.

Appendix. Supplementary data

Supporting information associated with this article can be found, in the online version, at doi:10.1016/j.polymer.2010.10.002.

References

[1] Luzinov I, Minko S, Tsukruk VV. Prog Polym Sci 2004;29:635–98.
[2] Ulbricht M. Polymer 2006;47:2217–62.
[3] Bergbreiter DE, Srinivas B. Macromolecules 1992;25:636–43.
[4] Qian H, Zhang YX, Huang SM, Lin ZY. Appl Surf Sci 2007;253:4659–67.
[5] Khayet M, Vàzquez Álvarez M, Khulbe KC, Matsuura T. Surf Sci 2007;601:885–95.
[6] Lee H, Archer LA. Macromolecules 2001;34:4572–9.
[7] Lee H, Archer LA. Polymer 2002;43:2721–8.
[8] Chen J, Gardella JAJ. Macromolecules 1998;31:9328–36.
[9] Kunz K, Anastasiadis SH, Stamm M, Schurrat T, Rauch F. Eur Phys J B 1999;7:411–9.
[10] Rimdusit S, Benjapan W, Assabumrungrat S, Takeichi T, Yokota R. Poly Eng Sci 2007;47:489–98.
[11] Tan J, Brash JL. J Appl Polym Sci 2008;108:1617–28.
[12] Oyane A, Ishizone T, Uchida M, Furukawa K, Ushida T, Yokoyama H. Adv Mater 2005;17:2329–32.
[13] Thomas HR, O'Malley JJ. Macromolecules 1978;12:323–9.
[14] Braunecker WA, Matyjaszewski K. Prog Polym Sci 2007;32:93–146.
[15] Ista LK, Pérez-Luna VH, López GP. Appl Environ Microbiol 1999;65(4):1603–9.
[16] Ito Y, Chen G, Guan Y, Imanishi Y. Langmuir 1997;13:2756–9.
[17] Cunliffe D, Alarcón CdlH, Peters V, Smith JR, Alexander C. Langmuir 2003;19:2888–99.
[18] Li L, Zhu Y, Li B, Gao C. Langmuir 2008;24:13632–9.
[19] Bandrup J. Polymer handbook. 3rd ed. New York: Wiley-VCH; 1989.
[20] Barton AFM. Handbook of polymer–liquid interaction parameters and solubility parameters. Boca Raton: CRC Press; 1990.
[21] Ahmad H. J Macromol Sci A 1982;17(4):585–600.
[22] Klibanov AM. J Mater Chem 2007;17:2479–82.
[23] Lewis K, Klibanov AM. Trends Biotechnol 2005;23(7):343–8.
[24] Queffelec J, Gaynor SG, Matyjaszewski K. Macromolecules 2000;33:8629–39.
[25] Berndt E, Ulbricht M. Polymer 2009;50:5181–91.
[26] Möckel D, Staude E, Dal-Cin M, Darcovich K, Guiver M. J Membr Sci 1998;145:211–22.
[27] Tiller JC, Liao C-J, Lewis K, Klibanov AM. Proc Natl Acad Sci U S A 2001;98(11):5981–5.
[28] Okano T, Yamada N, Sakai H, Sakurai Y. J Biomed Mater Res 1993;27:1243–51.
[29] Ista LK, López GP. J Ind Microbiol Biotechnol 1998;20:121–5.
[30] Gilcreest VP, Carroll WM, Rochev YA, Blute I, Dawson KA, Gorelov AV. Langmuir 2004;20:10138–45.
[31] Yakushiji T, Sakai K, Kikuchi A, Aoyagi T, Sakurai Y, Okano T. Langmuir 1998;14:4657–62.
[32] Lee SB, Koepsel RR, Morley SW, Matyjaszewski K. Biomacromolecules 2004;5:877–82.

[33] Huang J, Koepsel RR, Murata H, Wu W, Lee SB, Kowalewski T, et al. Langmuir 2008;24:6785–95.
[34] Park D, Wang J, Klibanov AM. Biotechnol Prog 2006;22:584–9.
[35] Lichter JA, Van Vliet KJ, Rubner MF. Macromolecules 2009;42:8573–86.
[36] Kurt P, Gamble LJ, Wynne KJ. Langmuir 2008;24:5816–24.
[37] Kügler R, Bouloussa O, Rondelez F. Microbiology 2005;151:1341–8.
[38] Murata H, Koepsel RR, Matyjaszewski K, Russel AJ. Biomaterials 2007;28:4870–9.
[39] Werner C, Jacobasch H-J, Reichelt G. J Biomater Sci Polym Edn 1995;7(1):61–76.
[40] Milovic MN, Wang J, Lewis K, Klibanov AM. Biotechnol Bioeng 2005;90(6):715–22.
[41] Haugland RP. A guide to fluorescent probes and labeling technologies. 10th ed.; 2005. Carlsbad: Invitrogen.
[42] Susanto H, Stahra N, Ulbricht M. J Membr Sci 2009;342:153–64.